Paradoxical androgen receptor regulation by small molecule enantiomers

Katherin Patsch[a,1] , Chao Liu[b,1] , Grzegorz Zapotoczny[a] , Yuanye Sun[b], Harish Sura[a], Nolan Ung[a] , Ren X. Sun[a], Bethany Haliday[a] , Chen Yu[a] , Mayada Aljehani[a] , Jerry S. H. Lee[a,c,d,e] , Boris A. Kashemirov[b] , David B. Agus[a,c,d] , Charles E. McKenna[a,b,d,2,3] , and Daniel Ruderman[a,c,d,2,3]

[a]Lawrence J. Ellison Institute for Transformative Medicine, University of Southern California, Los Angeles, CA 90064; [b]Department of Chemistry, Dana and David Dornsife College of Letters, Arts, and Sciences, University of Southern California, Los Angeles, CA 90089; [c]Department of Medicine and Oncology, Keck School of Medicine, University of Southern California, Los Angeles, CA 90033; [d]Norris Comprehensive Cancer Center, Keck School of Medicine, University of Southern California, Los Angeles, CA 90033; and [e]Department of Chemical Engineering and Material Science, Viterbi School of Engineering, University of Southern California, Los Angeles, CA 90089

Small molecules that target the androgen receptor (AR) are the mainstay of therapy for lethal castration-resistant prostate cancer (CRPC), yet existing drugs lose their efficacy during continued treatment. This evolution of resistance is due to heterogenous mechanisms which include AR mutations causing the identical drug to activate instead of inhibit the receptor. Understanding in molecular detail the paradoxical phenomenon wherein an AR antagonist is transformed into an agonist by structural mutations in the target receptor is thus of paramount importance. Herein, we describe a reciprocal paradox: opposing antagonist and agonist AR regulation determined uniquely by enantiomeric forms of the same drug structure. The antiandrogen BMS-641988, which has (R)-chirality at C-5 encompasses a previously uncharacterized (S)-stereoisomer that is, surprisingly, a potent agonist of AR, as demonstrated by transcriptional assays supported by cell imaging studies. This duality was reproduced in a series of novel compounds derived from the BMS-641988 scaffold. Coupled with in silico modeling studies, the results inform an AR model that explains the switch from potent antagonist to high-affinity agonist in terms of C-5 substituent steric interactions with helix 12 of the ligand binding site. They imply strategies to overcome AR drug resistance and demonstrate that insufficient enantiopurity in this class of AR antagonist can confound efforts to correlate structure with function.

androgen receptor | cancer | chirality | drug testing

Enzalutamide is the only Food and Drug Administration (FDA)-approved antiandrogen in metastatic castration-resistant prostate cancer (CRPC) (1), thus there is an urgent need for novel agents. Androgen receptor (AR) activation involves a cascade of events, including binding to the AR-ligand binding domain (AR-LBD) in the cytoplasm, nuclear translocation, and transactivation "hyperspeckling," where interaction with androgen response elements (AREs) regulates gene expression. These discrete steps can be measured via fluorescence polarization (2), confocal microscopy (3), and ARE-luciferase assays (4).

Agonist binding induces AR conformational changes that enable helix 12 (H12) to close the binding pocket, triggering activation (5). Establishing a predictive AR model for antagonists is hampered by the lack of structural information about AR bound to antagonist in open conformation. The AR antagonist BMS-641988 (6–8) has a chiral center at C-5 and an *endo* substituent [(R)-BMS]. Its unknown (S)-enantiomer [(S)-BMS] was postulated to also be an antagonist (7). When a new drug substance contains predominantly one enantiomer, its partner is excluded from the FDA's qualification and identification thresholds (9).

In this study of four BMS-641988 derivatives prepared as two enantiomeric pairs, we discovered that like (R)-BMS itself, the (R)-enantiomers [(R)-EITM-1702 and (R)-EITM-1707] were all AR antagonists. Unexpectedly, the corresponding (S)-enantiomers and (S)-BMS proved to be potent AR agonists.

Results and Discussion

Antagonist/Agonist Duality of Chiral Molecules. Initial compound testing was performed with PC3 GFP-AR cells and confocal microscopy. First, we tested purified BMS enantiomers (Fig. 1A). As expected (8), (R)-BMS was an antagonist: treatment initiated nuclear translocation but inhibited R1881-induced hyperspeckling. Surprisingly, (S)-BMS alone caused substantial hyperspeckling, comparable to that of R1881. To explore the significance of this result, which appeared to contradict literature inferences (7, 10), we prepared a series "EITM-17##" of cognate derivatives (Fig. 1B). Remarkably, their increased molecular size did not overcome paradoxical AR regulation. Nuclear spot quantification in >10,000 cells revealed all four (R)-enantiomers inhibited R1881-induced hyperspeckling, and their (S)-enantiomers induced it on their own (Fig. 1C). To test for corresponding transcriptional activation, we performed assays in cells expressing ARE-luciferase. (R)-enantiomers inhibited R1881-induced ARE-luciferase to 24% (95% CI = [18%, 34%]) vs. untreated R1881 control (no treatment control [NTC] + R1881, 100%) (Fig. 1D). In contrast, the (S)-enantiomers activated ARE-luciferase to 110% (95% CI = [87%, 130%]) of untreated control (NTC, 11%) (Fig. 1D). Next, we examined gene expression in VCaP cells, a hormone-responsive but -independent model of CRPC highly expressing AR. A qPCR array assaying 82 AR target genes in response to the natural hormone dihydrotestosterone (DHT) confirmed that (R)-EITM-1707 down-regulated AR-dependent gene expression, closely resembling androgen starvation. Its (S)-enantiomer rescued the castration phenotype, mimicking DHT (Fig. 1E). These experiments demonstrate enantiomer-dependent antagonist/agonist duality across these C-5 stereoisomers.

Model of AR-Enantiomer Duality. To explore the unexpected agonist properties of the (S)-enantiomers, we performed induced fit docking with the AR-LBD (PDB ID: 1E3G) (11) and (S)-EITM-1703. In the resulting model (rmsd = 0.28 Å), substituents do not clash with H12, but rather promote a closed conformation, which explains the observed agonism (Fig. 1F, AR in gray, compound in blue). Next, we sought to model the antagonist action of
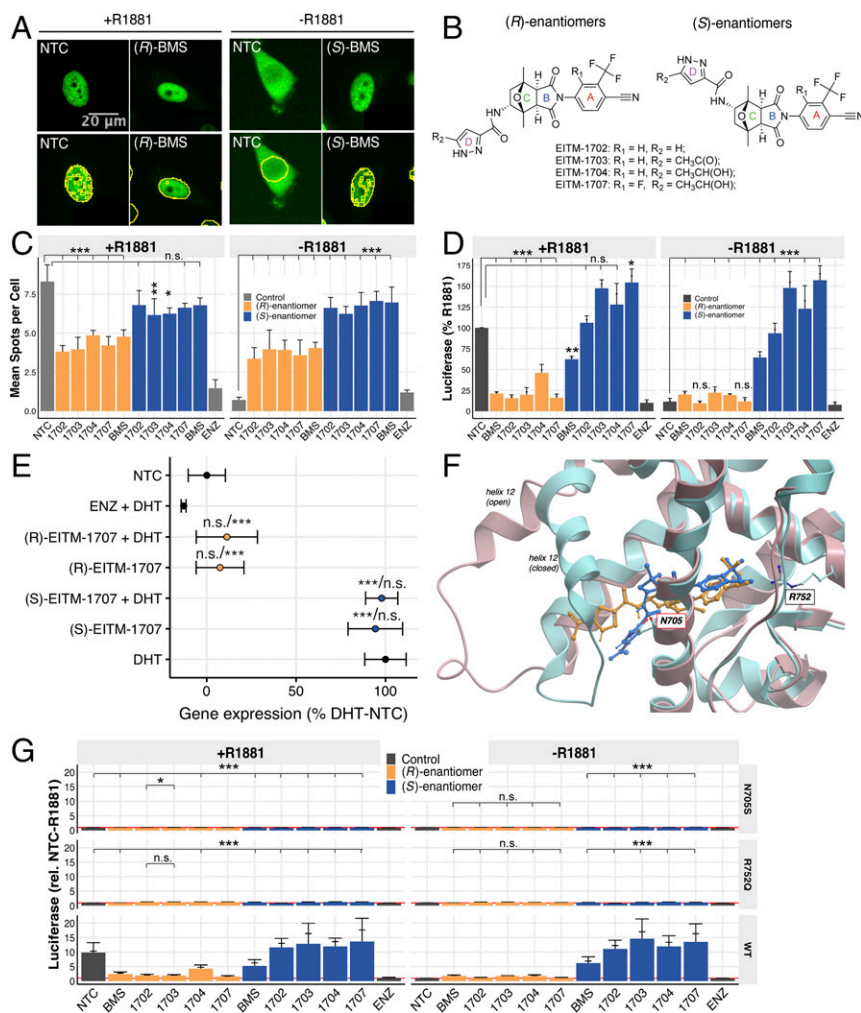
Fig. 1. Agonist/antagonist duality of enantiomers. (*A*) Confocal microscopy of PC3 GFP-AR cells treated with 10 µM purified enantiomers (180 min) and 1 nM R1881 (90 min). Representative cells are depicted. (*B*) Chemical structures of EITM-17## enantiomers. (*C*) Nuclear speckling quantification of EITM drug pairs. Data (*n* = 3 encompassing 11,188 cells) are mean ± SD (wide) and SE (narrow), linear model (two-sided) significance tests for difference from controls. (*D*) ARE-luciferase assays in cells treated with 10 µM drug + 1 nM R1881. Data (n ≥ 4) are mean ± SD, linear model (two-sided), (EITM-drugs + R1881) vs. R1881, and (− R1881) vs. NTC. (*E*) Expression of 82 AR-regulated genes in VCaP cells treated with EITM-1707 enantiomers via qPCR Array. Gene expressions were projected along the expression change vector between NTC (0%) and DHT (100%). Data (*n* = 3) are mean ± SD, ANOVA with post hoc correction, vs. NTC (*Left*) and DHT (*Right*). (*F*) Proposed model of AR antagonist/agonist duality. Overlay of (*S*)-EITM-1703 (blue) docked onto AR-LBD in closed conformation (turquoise), and (*R*)-EITM-1703 (gold) in open AR homology model (gray). (*G*) ARE-luciferase assays in cells expressing GFP-AR with point mutations to predicted binding sites and treated with 10 µM drug + 1 nM R1881. Data (n ≥ 3) are mean ± SD (wide) and SE (narrow), linear model significance tests for difference (relative to NTC − R1881) from WT AR and the corresponding mutation (corrected for multiple comparisons). NTC = no treatment control, ENZ = enzalutamide, DHT = dihydrotestosterone, (*R*)-BMS = BMS-641988 and its (*S*)-isomer (*S*)-BMS. *$P < 0.05$, **$P < 0.01$, ***$P < 0.001$, n.s., not significant. *P* values corrected for multiple comparisons at a familywise error rate of 0.05.

(*R*)-EITM-1703. Due to the absence of crystal structures of antagonist-bound AR in open conformation, we built a three-dimensional (3D) homology model based on that of the progesterone receptor (2OVM) (12) (Fig. 1*F*, AR in turquoise, compound in gold). Now, ring D obstructs H12, preventing closure. An overlay of the two models in Fig. 1*F* shows the strikingly different compound orientations within the pocket. In both cases, hydrogen bonds are formed with R752 and N705,* the same residues that bind DHT (13) and R1881 (11). We confirmed these critical binding sites in cells expressing point mutations that significantly reduced agonist functionality of both R1881 and (*S*)-enantiomers in our ARE-luciferase assay (Fig. 1*G*). Our AR model provides a rationale for the paradoxical agonism of the (*S*)-enantiomers, highlighting the importance of a specific, rigid spatial orientation of the ligand within the AR-LBD to ensure that antagonist function is not subverted to agonism. Future studies will systematically examine mutations within H12 that contribute to its steric interactions with the ligands.

Role of Enantiomer Duality in Drug Discovery. This new AR duality provoked the question whether agonistic enantiomer contamination could interfere with assays commonly used to identify new antiandrogens. To measure the impact of impurities after resolution, we spiked the highly purified (*R*)-enantiomers with their (*S*)-isomers and treated cells with 10 µM of the mixtures. For both

EITM-1702 and EITM-1707, ARE-luciferase signals rapidly increased with increasing levels of contamination (Fig. 2*A*). For (*S*)-EITM-1702, 2.5% contamination (95% CI = [2.1%, 2.9%]) halved the drug effect, and 9% (95% CI = [6%, 12%]) canceled out its antagonist effect entirely (Fig. 2*A*). The contamination effect was even more detrimental on cell viability measured via CellTiter-Glo. After 6-d treatment, pure (*R*)-EITM-1702 and (*R*)-EITM-1707 visibly suppressed R1881-induced growth, whereas BMS-641988 did not (Fig. 2*B*). Strikingly, as little as 0.3% (*S*)-enantiomer halved EITM-1702 drug effect (95% CI = [0.2%, 0.4%]), and 2.2% rescued the proliferation phenotype (95% CI = [0.7%, 3.7%]) (0.7%, 3.7%) 95% CI (Fig. 2*B*). Furthermore, agonist EC$_{50}$ values obtained by fluorescence polarization and ARE-luciferase were consistently lower than their respective antagonist counterparts, suggestive of higher affinity (Fig. 2*C*) and potency (Fig. 2*D*). These experiments reveal the critical importance of enantiopurity in this drug class, even during early discovery when antagonist "hits" could be otherwise missed or even misidentified as agonists.

Materials and Methods

Cell Culture and Treatments. PC3 and VCaP cell lines were obtained from ATCC and cultured as recommended. Generation and culture of PC3 GFP-AR cells were described previously (14). ARE-luciferase cells were generated using Cignal Lenti AR Reporter (Qiagen). Cell lines were authenticated using National Institute of Standards and Technology-approved short tandem repeat DNA profiling and tested negative for mycoplasma. Drug treatments were conducted after overnight culture in phenol red-free media supplemented with charcoal:dextran stripped fetal bovine serum.
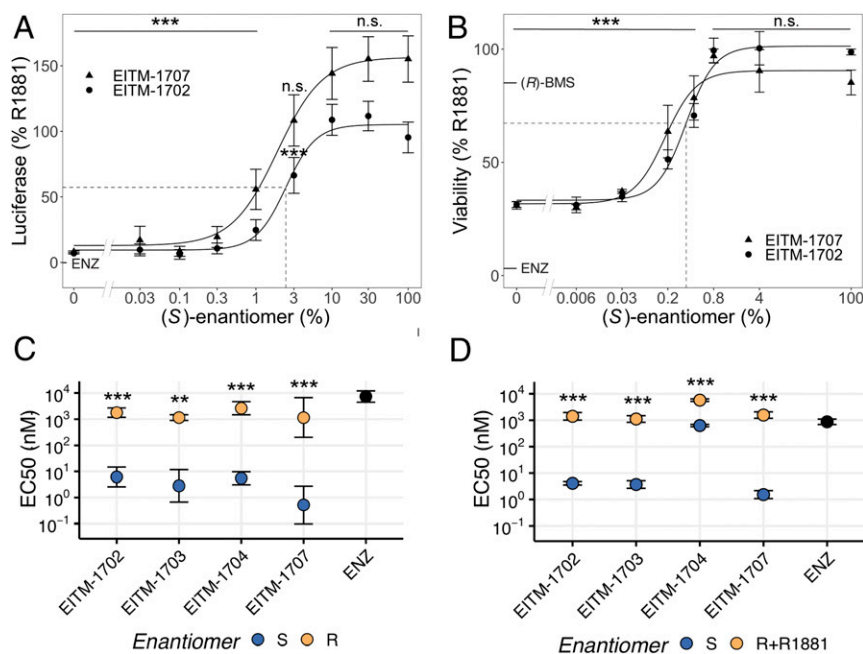
---

*Nomenclature of GenBank mRNA sequence M20132.1.

Fig. 2. Role of enantiomer duality in in vitro drug testing. (*A* and *B*) Assays in cells treated with 10 μM drug with increasing fractions of (*S*)-enantiomer + 1 nM R1881. (*A*) ARE-luciferase was measured after 24 h and (*B*) VCaP cell viability after 6 d of treatment using CellTiter-Glo. Data (n = 3) are mean ± SD, one-sided Wilcoxon test for decrease from R1881 across both drugs. Dashed lines represent relative EC_{50} for EITM-1702. Zero% data points were not used to fit the curves. (*C* and *D*) Pairwise EC_{50} values computed from (*C*) competition binding curves obtained via fluorescence polarization and (*D*) ARE-luciferase dose–response curves run in antagonist mode (1 nM R1881) with (*R*)-drugs and in agonist mode (−R1881) with their respective (*S*)-isomers. Data (n ≥ 3) are mean ± SD, two-sided Welch *t* test, **$P < 0.01$, ***$P < 0.001$, n.s., not significant. NTC = no treatment control, ENZ = enzalutamide.

Confocal Microscopy. PC3 GFP-AR cells were seeded and stained overnight with SiR-DNA (Cytochrome). Cells were treated 180 min with drug and 90 min with ligand and imaged on an Operetta CLS microscope (PerkinElmer).

Luminometer Assays. For ARE-luciferase, luciferase substrate was added to lysed cells after 24-h treatment. For viability, cells were lysed with CellTiter-Glo 3D Cell Viability Assay (Promega) after 6 d of treatment. Measurements were performed in 96-well plates (Corning) using a GloMax 96 Microplate Luminometer (Promega).

AR Binding. Ligand binding was analyzed using the PolarScreen AR Competitor Assay Kit, Green, according to the manufacturer's instructions (Thermo Fisher Scientific). Fluorescence polarization was measured after a 4-h incubation using an EnVision 2103 Multilabel Plate Reader (PerkinElmer).

RT-qPCR Array. RNA was isolated using the Illustra RNAspin Mini Kit (GE Healthcare). RNA was transcribed to cDNA using RT2 First Strand Kit (Qiagen).

RT-qPCR was performed using Biorad CFX Connect on a RT2 Profiler PCR Array Human Androgen Receptor Signaling Targets (Qiagen).

Molecular Docking and Induced Fit. Agonist docking was performed with the WT-AR-LBD (PDB ID: 1E3G) in complex with R1881 using Schrodinger Suite 2018–3 (Glide, Prime). For antagonists, a homology model of WT-AR-LBD in open conformation was built with Schrodinger Prime using the progesterone receptor (PDB ID: 2OVM) as a template.
SI Appendix provides extended methods.

1. P. A. Watson, V. K. Arora, C. L. Sawyers, Emerging mechanisms of resistance to androgen receptor inhibitors in prostate cancer. *Nat. Rev. Cancer* **15**, 701–711 (2015).
2. W. Zhou *et al.*, Discovery of novel androgen receptor ligands by structure-based virtual screening and bioassays. *Genomics Proteomics Bioinformatics* **16**, 416–427 (2018).
3. C.-L. Chiu *et al.*, Intracellular kinetics of the androgen receptor shown by multimodal Image Correlation Spectroscopy (mICS). *Sci. Rep.* **6**, 22435 (2016).
4. A. T. Szafran, M. Szwarc, M. Marcelli, M. A. Mancini, Androgen receptor functional analyses by high throughput imaging: Determination of ligand, cell cycle, and mutation-specific effects. *PLoS One* **3**, e3605 (2008).
5. M. H. Tan, J. Li, H. E. Xu, K. Melcher, E. L. Yong, Androgen receptor: Structure, role in prostate cancer and drug discovery. *Acta Pharmacol. Sin.* **36**, 3–23 (2015).
6. D. Rathkopf *et al.*; Prostate Cancer Clinical Trials Consortium, Phase I dose-escalation study of the novel antiandrogen BMS-641988 in patients with castration-resistant prostate cancer. *Clin. Cancer Res.* **17**, 880–887 (2011).
7. A. Balog *et al.*, Discovery of BMS-641988, a novel androgen receptor antagonist for the treatment of prostate cancer. *ACS Med. Chem. Lett.* **6**, 908–912 (2015).
8. R. M. Attar *et al.*, Discovery of BMS-641988, a novel and potent inhibitor of androgen receptor signaling for the treatment of prostate cancer. *Cancer Res.* **69**, 6522–6530 (2009).
9. Food and Drug Administration, HHS, International conference on harmonisation; guidance on Q6A specifications: Test procedures and acceptance criteria for new drug substances and new drug products: Chemical substances. Notice. *Fed. Regist.* **65**, 83041–83063 (2000).
10. M. E. Salvati *et al.*, Identification and optimization of a novel series of [2.2.1]-oxabicyclo imide-based androgen receptor antagonists. *Bioorg. Med. Chem. Lett.* **18**, 1910–1915 (2008).
11. P. M. Matias *et al.*, Structural evidence for ligand specificity in the binding domain of the human androgen receptor. Implications for pathogenic gene mutations. *J. Biol. Chem.* **275**, 26164–26171 (2000).
12. K. P. Madauss *et al.*, A structural and in vitro characterization of asoprisnil: A selective progesterone receptor modulator. *Mol. Endocrinol.* **21**, 1066–1081 (2007).
13. J. S. Sack *et al.*, Crystallographic structures of the ligand-binding domains of the androgen receptor and its T877A mutant complexed with the natural agonist dihydrotestosterone. *Proc. Natl. Acad. Sci. U.S.A.* **98**, 4904–4909 (2001).
14. K. Patsch *et al.*, Single cell dynamic phenotyping. *Sci. Rep.* **6**, 34785 (2016).
15. K. Patsch *et al.*, Paradoxical androgen receptor regulation by small molecule enantiomers. Zenodo. https://zenodo.org/record/4148931. Deposited 5 March 2021.

Patsch et al.
Paradoxical androgen receptor regulation by small molecule enantiomers

PNAS | 3 of 3
https://doi.org/10.1073/pnas.2100918118